Neuroscience 222 (2012) 228–238

THE CHARACTERIZATION OF ARACHNOID CELL TRANSPORT II: PARACELLULAR TRANSPORT AND BLOOD–CEREBROSPINAL FLUID BARRIER FORMATION

C. H. LAM,[a,b,c*] E. A. HANSEN,[c1] C. JANSON,[b2] A. BRYAN[c3] AND A. HUBEL[a4]

[a] *Department of Biomedical Engineering, University of Minnesota, Minneapolis, MN, United States*

[b] *Department of Neurosurgery, University of Minnesota, Minneapolis, MN, United States*

[c] *Minneapolis Veterans Administration Medical Center, Minneapolis, MN, United States*

Abstract—We used an immortalized arachnoid cell line to test the arachnoid barrier properties and paracellular transport. The permeabilities of urea, mannitol, and inulin through monolayers were 2.9 ± 1.1 × 10^{-6}, 0.8 ± .18 × 10^{-6}, 1.0 ± .29 × 10^{-6} cm/s. Size differential permeability testing with dextran clarified the arachnoidal blood–cerebrospinal fluid (CSF) barrier limit and established a rate of transcellular transport to be about two orders of magnitude slower than paracellular transport in a polyester membrane diffusion chamber. The theoretical pore size for paracellular space is 11 Å and the occupancy to length ratio is 0.8 and 0.72 cm^{-1} for urea and mannitol respectively. The permeability of the monolayer was not significantly different from apical to basal and vice versa. Gap junctions may have a role in contributing to barrier formation. Although the upregulation of claudin by dexamethasone did not significantly alter paracellular transport, increasing intracellular cAMP decreased mannitol permeability. Calcium modulated paracellular transport, but only selectively with the ion chelator, EDTA, and with disruption of intracellular stores. The blood–CSF barrier at the arachnoid is anatomically and physiologically different from the vascular-based blood–brain barrier, but is similarly subject to modulation. We describe the basic paracellular transport characteristics of this CSF ''sink'' of the brain which will allow for a better description of mass and constitutive balance within the intracranial compartment. Published by Elsevier Ltd. on behalf of IBRO.

Key words: cerebrospinal fluid, hydrocephalus, arachnoid, blood–CSF barrier, blood–brain barrier.

INTRODUCTION

Cerebrospinal fluid (CSF) is important for the central nervous system's support and maintenance. It buffers the nervous tissues mechanically and chemically, serves as a vehicle for the transport of important substances, and removes waste and debris (Carpenter, 1991). Arachnoidal CSF egress is considered one of the major routes of CSF removal (Upton and Weller, 1985). How this occurs is unknown, but given the aqueous nature of CSF, the primary mean is thought to be paracellular transport. Paracellular transport is governed by a variety of mechanisms and components: cell height, paracellular space tortuosity, tight junctions, and gap junctions, of which the tight junction may be the most crucial. As a major component of the blood–CSF barrier (BCB) and ''sink'' for CSF absorption, the arachnoid stands at an important junction between the vascular system and the intracranial space. This gateway is similar to the blood–brain barrier (BBB) in that polar substances and dyes are restricted in their movement (Wolpow and Schaumburg, 1972). Arachnoidal tissue exists in multiple forms including membranes, dense granulation caps, and porous central cores (Kida et al., 1988). The degree of intracellular or extracellular matrix pathway involvement in transport is probably dependent on this local structure of the arachnoid tissue, but preliminary tracer studies have shown that permeabilities of low molecular weight substances in confluent monolayers parallel that of the BBB (Holman et al., 2010; Lam et al., 2011). Tight junctions crucial to the integrity of the BCB and regulation of paracellular transport have also been seen in the arachnoid cell–cell contacts with transmission electron microscopy (Hasegawa et al., 1997). Holman recently demonstrated these junctional complexes on cultured arachnoid monolayers as well. These complexes maintain the pathway integrity in conditions of osmotic and pressure gradient challenges. The geometric path and the chemical makeup in the paracellular space could be altered during these conditions, regulating the outflow of fluid out of the brain

*Corresponding author. Address: University of Minnesota MMC 96, 420 Delaware Street, S.E. Minneapolis, MN 55455, United States. Tel: +1-612-624-5433; fax: +1-612-624-0644.
E-mail addresses: lamxx023@umn.edu (C. H. Lam), hanse989@umn.edu (E. A. Hansen), hubel001@umn.edu (A. Hubel).
[1] Department of Surgery, Minneapolis Veterans Administration Hospital, 1 Veterans Drive, Minneapolis, MN 55417, United States. Tel: +1-612-467-4702.
[2] Department of Neurosurgery, University of Minnesota, MMC 96, 420 Delaware Street, S.E. Minneapolis, MN 55455, United States. Tel: +1-612-624-5433.
[3] Department of Surgery, Minneapolis Veterans Administration Hospital, 1 Veterans Drive, Minneapolis, MN 55417, United States. Tel: +1-612-624-5433.
[4] Department of Mechanical Engineering, University of Minnesota, 111 Church Street, S.E. Minneapolis, MN 55455, United States. Tel: +1-612-626-4451.
Abbreviations: BBB, blood–brain barrier; BCB, blood–CSF barrier; CSF, cerebrospinal fluid; EDTA, ethylenediaminetetraacetic acid.

0306-4522/12 $36.00 Published by Elsevier Ltd. on behalf of IBRO.
http://dx.doi.org/10.1016/j.neuroscience.2012.06.065

and the intracranial cavity probably by a combination of complex feedback systems involving second messengers and physical alterations in the cells.

Because of the similarities in permeabilities of ionic substances in arachnoid cell-mediated blood–CSF barrier and BBB, the demonstration of regulated flow through the arachnoid cell, and the importance of arachnoid cells in the removal of CSF from the brain, we characterize in detail the paracellular transport in an immortalized cell line of the arachnoid cells (see (Janson et al., 2011) for cell line description) and investigate the physiologic mechanisms that alter this transport in this paper. Two important mechanisms in tight junction regulation are the calcium and cAMP second messenger pathways (Karczewski and Groot, 2000; Deli, 2009). They regulate the various intercellular junctional proteins, such as claudin, as well as the intracellular cytoskeletal systems important for transport. Given the cell's barrier capabilities, we expect the cellular and molecular dynamics to be similar to the BBB. However, an overarching element of contrast between the arachnoid cells and the brain endothelial cells is that the "neurovascular unit" is absent (see (Hawkins and Davis, 2005) for review). Lacking the astrocytic, neuronal, and pericytic influences on the BBB junctional complex, we believe the mechanisms of the BCB maintenance to be under different control and regulation. To that end, we believe the control mechanisms to be simpler and to be less finely controlled. Therefore, we probe the junctional complexes in arachnoid monolayers directly and test its integrity with well-known second messenger perturbation methods in these sets of experiments.

EXPERIMENTAL PROCEDURES

Production of retrovirus containing SV40 LgTAg and hTERT and retroviral transduction

The generation of immortalized arachnoid cells has been previously presented.(Janson et al., 2011) Briefly, the retroviral constructs pBABE-neo-hTERT and pBABE-puro-SV40LT, containing hTERT and SV40 LTAg along with the G418 and puromycin resistance genes, were used to transfect the EcoPack2 cells (Clontech Mountain View, CA), which are 293HEK ecotropic feeder cells containing retroviral packaging genes. Cells were seeded 12–18 h prior to use at 5×10^5 cells in 25 cm^2 flasks. Then 5 mg of pBABE-puro-SV40LT was combined with the Fugene reagent (Roche Indianapolis, IN) and the OptiMem (Invitrogen) serum-free media in 250 ml total reaction volume with 3:1 ratio of Fugene:DNA. This was incubated for 30 min and added to each flask of 293HEK ecotropic feeder cells, with 3 ml of serum-containing media per flask.

Arachnoid cells were harvested from 21-to 23-day old male Sprague–Dawley rats. At passages 3 or 4, the arachnoid cells were replated into a Biocoat six-well plate (BD Biosciences San Jose, CA). Viral transduction was performed when the cells reached 60–80% confluence. Clarified viral supernatant containing BABE-puro-SV40LT was applied sequentially to the arachnoid cell primary culture. Target cells were initially at a density of 4×10^4 cells per well of a six-well plate. The media was aspirated and 3 ml virus-containing media was added per well. Polybrene (Millipore) was then added to a final concentration of 4 mg/ml. Cells transduced with pBABE-puro-SV40LT were selected over 14 days with puromycin (Sigma).

Histology and immunohistochemistry

Cells were permeabilized in 0.25% Triton X-100, blocked in 2% bovine serum albumin, and incubated with primary antibodies in PBS overnight at 4 °C. After rinsing with PBS (phosphate buffered saline), cells were incubated with appropriate secondary antibody and counterstained with DAPI. Images were analyzed using a Biorad MRC-1024 single photon confocal microscope 1024 (Biorad Cell Science, UK) (see Lam et al., 2011 for complete staining procedures). For establishing the presence of junctional proteins, the cells were stained with Claudin-1 (prod # RB-9209-PO, Thermo Scientific, West Palm Beach, FL) , connexin 45 (Prod #MAB3100, Millipore, Billerica, MA), ZO-1 (prod # ab59720 Abcam Inc., Cambridge, MA), and JAM-A (prod # 361700, Invitrogen, Carlsbad, CA). Actin (prod # 4970 Cell Signaling Technology, Danvers, MA) staining was also performed to show the cytoskeletal filaments.

TEM

The arachnoid cells were fixed on Transwell membranes with 3% glutaraldehyde solution in 0.1 M phosphate buffer. After glutaraldehyde fixation, the cells were postfixed in 1% osmium tetroxide in 0.1 M phosphate buffer containing 0.1 M sucrose (pH 7.4). They were then rinsed, stained (1% uranyl acetate overnight at 4 °C), and dehydrated in a graded series of ethanol.

The samples were incubated in two changes of hydroxypropyl methacrylate and placed in 100% resin overnight (Polybed 816), then embedded in fresh resin (Polybed 812; both from Polyscience, Warrington, PA) in a round silicon mold and polymerized at 60 °C for 24 h. The embedded samples were sectioned on an ultramicrotome (EM UC6; Leica) at 70 nm and stained with 2% uranyl acetate and Reynolds lead citrate. Samples were examined under a transmission electron microscope (Philips CM12 Transmission Electron Microscope) and photos taken with SIA L3C Digital Camera.

Functional transport assay: TEER, marker, and size differential transport study

4×10^5 immortalized rat arachnoid cells were plated in each of the 3 top wells of a 6-well Transwell (Corning Inc. Corning, NY; Cat No. 3450) (4.67 cm^2 per well and 0.4 μm pore size), and incubated for 3–5 days depending on when the cells became confluent. Three blank Transwells were used as negative controls. Separate 24-well plates Transwell (Corning Inc. Corning, NY; Cat No. 3470) (0.3 cm^2 per well and 0.4 μm pore size) were used for TEER (Trans Epithelial Electric Resistance) studies. Cells were plated at 3×10^4 cells per well and grown to confluency. Culture media in Transwell plates was removed and pre-warmed media was added into wells (apical 2 ml, basolateral 3 ml). The ^{3}H-mannitol stock solution was prepared as 1 ml radiolabeled mannitol per 1000 ml of assay buffer [LR1], for a final mannitol concentration of 82 nm and specific activity of 1 mCi/ml. The buffer was removed from the proximal (apical) compartments and pre-warmed radioactive solution was added to apical chambers, with 2 ml to each chamber. The plate was put on gentle shaker at 37 °C and 200 μl samples were taken from both compartments in each well at 15, 30, 60, 90, 120 min and replaced with an equal volume of respective buffer. Inulin-[Carboxyl-^{14}C] (50 mCi/mmol, Fisher Scientific Inc. Cat #1108650) and [^{14}C] Urea (54 mCi/mmol, Amersham, Piscataway NJ) were prepared as 1 ml of radiolabeled compound per 1000 ml assay buffer and tested in the same fashion. For the FITC (Fluorescein isothiocyanate)-labeled Dextran (10, 20, 40, and 70 kDa) (Cat No. 129K5304, 83797PJ, 069K5316. Sigma–Aldrich Co., St. Louis, MO) experiment, 1×10^5 immortalized rat arachnoid cells were seeded and tested in the same paradigm. All of the signals were measured

using a Packard SpectraCount photometric microplate reader (measured at 520 nm) (Packard Instrument Co., Meriden, CT) with control plates subtracted out. The TEER studies were performed using a transepithelial voltmeter (World Precision Instruments) according to the manufacturer's recommendations. The TEER value of a blank membrane was subtracted from the apparent TEER values of membranes with cells to obtain the effective TEER value.

The amount of tracer crossing the monolayer was reported as the arachnoid permeability ($P_{\text{arachnoid}}$, cm/s). The cleared volume was calculated by dividing the concentration in the receiver compartment by the product concentration in the donor compartment at each time point. Average cumulative volume cleared was plotted versus time and the slope was estimated by linear regression analysis to give the mean and the standard deviation of the estimate. The P value for the arachnoid monolayer alone was obtained as follows: $1/P_{\text{arachnoid overall}} = 1/P_{(\text{recorded})} - 1/P_{\text{insert}}$. To generate the permeability coefficient of the arachnoid cells, $P_{\text{arachnoid}}$ (cm/s) and $P_{\text{arachnoid overall}}$ values were divided by the surface area of the insert.

The theoretical pore size for neutral permeants was determined using the Renkin molecular sieving function, which uses the molecular radius (r) of the tracer and a cylindrical pore radius to model the paracellular space. (Knipp et al., 1997) The molecular radii are estimated using the Stokes–Einstein Law for equivalent spheres, which for mannitol and urea radii are 4.10 and 2.67 Å respectively. Solute pairing allows for the aqueous pore radius calculation from the paracellular permeability ratio thus:

$$\frac{P_x}{P_y} = \frac{r_y F\left(\frac{r_x}{R}\right)}{r_x F\left(\frac{r_y}{R}\right)}$$

where the hindrance function is defined thus:

$$F\left(\frac{r}{R}\right) = \left(1 - \left(\frac{r}{R}\right)\right)^2 \left[1 - 2.104\left(\frac{r}{R}\right) + 2.09\left(\frac{r}{R}\right)^3 - 0.95\left(\frac{r}{R}\right)^5\right]$$

The pore occupancy to length ratio (ε/L) as a characteristic value of the theoretical pore size is calculated using mannitol and urea using this equation (Seki et al., 2006):

$$P_x = \frac{\varepsilon}{L} D_x F\left(\frac{r_x}{R}\right)$$

where D is the diffusion coefficient and subscript, x, indicates either mannitol or urea.

Perturbation methods

Viability studies. The arachnoid cells were subjected to the maximal concentrations of drugs to determine survivability using the Live/Dead viability/cytotoxicity kit (Invitrogen). Live cells show diffuse cytoplasmic green fluorescence and dead or dying cells show nuclear red fluorescence. The cells show similar survivability to control during period of permeability measurements.

Junctional complex disruption (tight junctions), protamine. Protamine (MP Biomedicals, Solon, OH) diluted in PBS (BioWhittaker, Walkersville, MD) and buffered in Krebs–Ringer (27.4 mM NaCl, 1 mM KCl, 0.2 mM $MgSO_4 \cdot 7H_2O$, 0.06 mM KH_2PO_4, 0.06 mM $NaH_2PO_4 \cdot H_2O$, 2.8 mM Trizma base, 0.56 mM $CaCl_2 \cdot 2H_2O$, and 1.8 mM glucose) was added to the culture media to a final concentration of 10 mg/ml (pH 7.4, adjusted with HCl after protamine addition) (Skinner et al., 2009). The culture media bathing the monolayers was gently withdrawn and replaced by the buffered protamine to both the apical and basolateral compartments. The control buffer solution not containing the polycation was delivered in the same volume.

Junctional complex disruption (tight junctions), serum free conditions. Cells were passaged onto wells containing serum-free media for at least 3 days. Cell viability in serum-free conditions was first verified with qualitative assessments of growth and cell morphometry. When cells in both serum-free and serum-containing media were in confluency, TEER values were recorded and permeability measurements performed.

Junctional complex disruption (tight junctions), Dexamethasone studies. The cells were treated with dexamethasone (Sigma Aldrich, St. Louis, MO) at a concentration of 10 μM. After 24 h, the permeability of cells was performed by taking measurements every hour for 8 h. The cells receiving the control buffer solution were measured during the same time periods. Given the potential mechanism of steroids on protein induction, the experiments were repeated 3 days after being subjected to dexamethasone. TEER was measured over 10 days at concentrations of 1, 5, and 10 μM of dexamethasone.

Junctional complex disruption (gap junctions) 18β-glycyrrhetinic acid studies. To determine whether gap junctions contribute to the paracellular pathway, TEER and mannitol measurements were performed on cells treated with connexin disruptor, 18β-glycyrrhetinic acid (18β-GA) (Fisher Scientific, Fair Lawn, NJ). Confluent cells were treated for 30 min of 20 mM 18β-GA or vehicle. The exposure time and the concentration were determined from dose-and time-response curves. The timing of transport studies was determined from temporal data gathered from serial TEER values measured at 5 min intervals for 90 min at concentrations of 1, 5, 10, 20, and 40 mM 18β-GA.

Second messengers, calcium

Extracellular calcium was investigated using ethylenediaminetetraacetic acid, EDTA (MP Biomedicals, Solon, OH), as a chelator at 20 mM concentration. Permeability studies were performed at maximal effective dose as determined by the dose-response curve for the arachnoid cells at 15 min after treatment initiation. The dosing and the timing for transport studies was determined from the temporal data gathered from serial TEER values measured at 5 min intervals for 90 min at concentrations of 1, 5, 10, 20, and 40 mM EDTA. Using WebMaxC with temperature setting of 37 °C, pH = 7.3, and ionic strength of 0.165, free calcium concentration was calculated to vary from .6 to 1.5×10^{-6} mM.(Patton, 2011) Experiments were repeated with EGTA as it is a more potent chelator for calcium compared to magnesium. TEER results were identical at similar chelator concentration validating calcium effects (results not shown). Calcium was also increased in the culture media to a concentration of 4 mM from 1.66 mM. Intracellular calcium was perturbed in two ways. Intracellular calcium was decreased by using the calcium channel blocker, verapamil (MP Biomedicals, Solon, OH), at a concentration of 5 μM (Sakai et al., 1994). Intracellular calcium was also increased by using a calcium ionophore, ionomycin at concentration of 10 μM (Calbiochem, La Jolla, CA) (0.0015%w/v).

Second messengers, cAMP

cAMP (Sigma Aldrich, ST. Loius, MO) was added directly into the culture media at a concentration of 10 μM. Intracellular cAMP was perturbed using three different mechanisms. Adenylyl cyclase was augmented directly by forskolin (MP Biomedicals, Solon OH), (50 μM) (Liu et al., 1997), and indirectly through G protein induction with isoproterenol (Sigma–Aldrich, St. Louis, MO) (10 μM) (Izevbigie et al., 2000). cAMP breakdown was also inhibited by using rolipram (MP Biomedicals, Solon, OH) (10 μM), a phosphodiesterase type 4 inhibitor (Wigham et al.,

2000). Synergistic and cAMP ceiling effects of the drugs were studied using forskolin/isoproterenol, rolipram/isoproterenol, and rolipram/forskolin in combination.

RESULTS

Junctional protein expression

Previously we have demonstrated the arachnoid phenotype in these cells (Janson et al., 2011). We now examined the proteins most important in the barrier development in the immortalized arachnoid cell line. The immunoreactivity for ZO-1 and claudin indicates the presence of tight junctions (Fig. 1). This adds to our previous report of desmoplakin immunopositivity, indicating both desmosomal and tight junction cell-cell attachments. The tight junction proteins are marginated at edge of the cell abutting next to adjacent cells. Confluent cells in monolayers show polygonal morphology and are cobblestone in appearance. Connexin immunopositivity indicates that gap junctions were also present. Previous demonstrations of vimentin and cytokeratin intermediate filaments are complemented now by actin positivity which extends to junctional zones. This is in keeping with their role as intracellular links to the tight junction (Fig. 1).

Marker and size differential studies, A to B and B to A

Mannitol, urea, and inulin were used as classic benchmarks for paracellular transport in this arachnoid cell line (Fig. 2A–C). Using uncoated polyester filter with confluent monolayers, we determined first stable TEER values and consistent permeability coefficients and then compared them to primary cell coefficients as well as caco-2 as control model. The results of the basic transport characteristics of the cells are summarized in Table 1. Permeabilities of the classic markers of barrier inulin, mannitol, and urea were $1.0 \pm .29 \times 10^{-6}$, $0.8 \pm .18 \times 10^{-6}$, $2.9 \pm 1.1 \times 10^{-6}$ cm/s ($\pm$ indicates S.E.) respectively, which were similar to primary cell cultures. In addition, cells demonstrated molecular size delimited differences in barrier separation when we use 10-, 20-, 40-, and 70-kDa FITC-dextran as tracers with stepoff between the 10 and 40 kDa range. The monolayers were studied with tracers placed in the basolateral (B) side and apical (A) side. (Fig. 2D, E) Directionality was not statistically different suggesting a non-intracellular mechanism of transport (Fig. 2F) and is consistent with paracellular movement.

Pore size and pore occupancy

Using the Renkin hindrance function for mannitol and urea, the theoretical pore size is calculated to be 11 Å and the occupancy to pore length ratio to be 0.7–0.8 cm^{-1}. Others have shown that the anionic forms of tracers tend to have lower permeabilities than those of equivalent molecular weight in caco2 cells (Knipp et al., 1997), when using inulin (p*Ka* = 6), the permeability plateaued to the same level as mannitol. This could be due to wider paracellular space of arachnoid and the mild acidity of inulin.

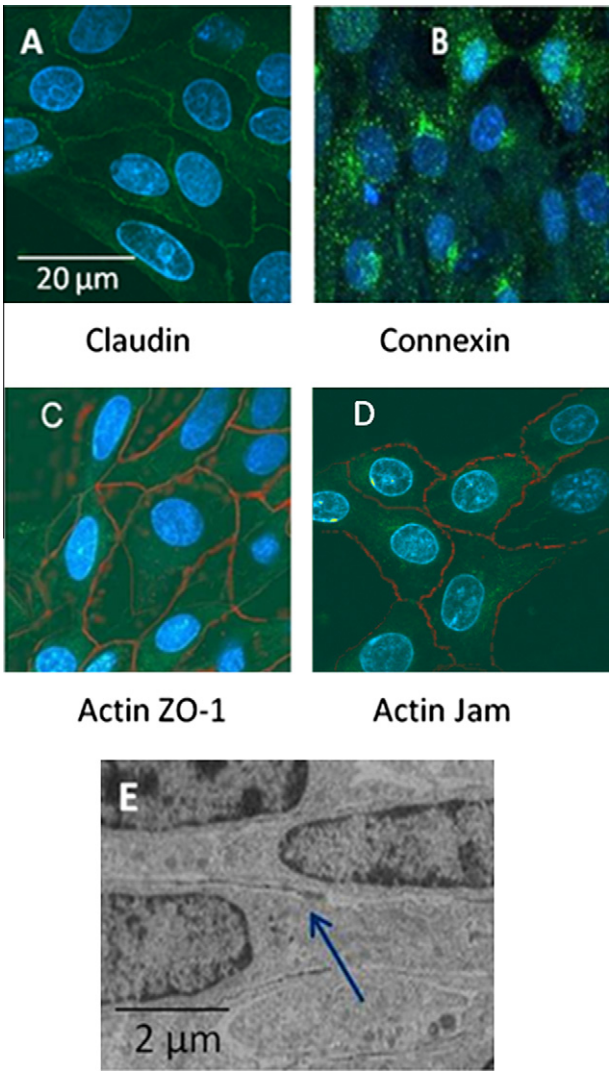

Fig. 1. Junctional protein immunohistochemistry, transmission electron microscopy, and actin staining. (A) Immunostaining for claudin-1 (green) demonstrates the margination of the protein along the edge of the cell in contact with adjacent cell. (B) Punctate staining (green) of connexin is consistent with the presence of gap junctions. (C) Double staining for actin and ZO-1. Filamentous appearance of actin cytoskeletal protein (green) is seen as well as the second tight junctional protein, ZO-1, along the periphery (red). (D) JAM (red), a third component of tight junctions seen along the margin of the cell co-localizes with the same cells manifesting actin (green) intracellularly. DAPI for nuclear staining is blue on all panels. Scale is identical on panels A to D. (E) Transmission electron microscopy demonstrating tight junction (arrow) forming between adjacent cells. Scale bar = 2 µm.

Perturbation studies

Junctional proteins modulation (tight junctions and gap junctions). Tight junctions. We studied the tight junctions directly using three means of perturbation: serum-free media, protamine and dexamethasone. Serum-free conditions disrupt paracellular transport by altering the tight junctional zonula occludens protein (Hakvoort et al., 1998), while protamine affects the tight

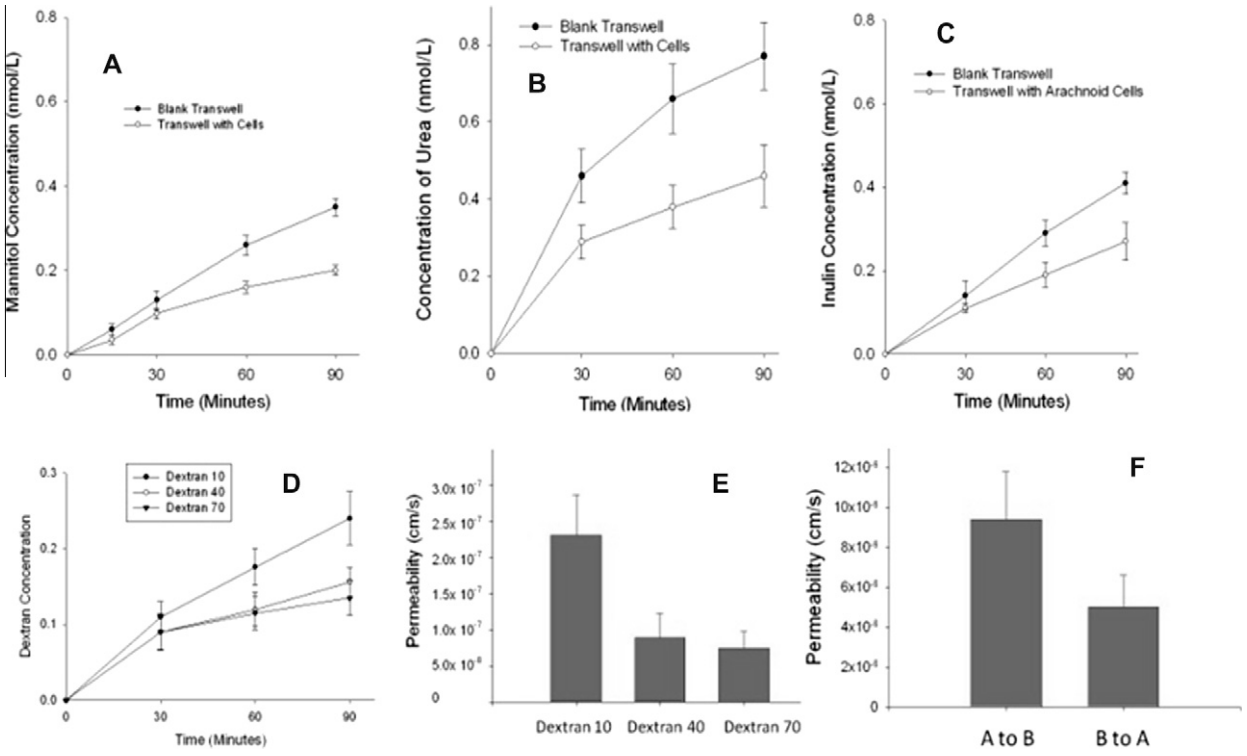

Fig. 2. Paracellular marker and size differential studies. Permeation studies for standard paracellular tracers, (A) mannitol, (B) urea, (C) inulin. ($n = 5$ for each, error bars denote S.E.) (D) Permeability curves for FITC dextran, and (E) Bar graph demonstrating steep decrease in permeability around molecular weight of 10,000. Permeability of small tracers is one order of magnitude higher than FITC-dextran 10. (F) Directionality of cell line monolayer from apical to basal and basal to apical is not statistically different. Permeabilities were $5.2 \times 10^{\wedge} - 6$ cm/s for B to A S.E. 1.3 and $9.8 \times 10^{\wedge} - 6$ cm/s for A to B S.E. 2.4, paired *t*-test, $p = .065$.

Table 1. Tracer characteristics of arachnoid.

	m.w.	F (r/R)	P (cm/s)	ε/L (cm^{-1})	D (cm^2/s)	R (Å)	p*Ka*
Urea	60	.297	$2.9 \pm 1.1 \times 10^{-6}$	.80	1.22×10^{-5} (S–E eqn*)	2.67 (Adson et al., 1994)	Neutral
Mannitol	182	.125	$0.8 \pm .18 \times 10^{-6}$	.72	8.9×10^{-6} (S–E eqn, (Lanman et al., 1971)	4.10 (Adson et al., 1994)	Neutral
Inulin	5000–5500		$1.0 \pm .29 \times 10^{-6}$		2.9×10^{-6} (S–E eqn, (Lanman et al., 1971)	15 (Al-Sadi et al., 2011) 11 (Lanman et al., 1971)	6.33
FITC-dextran 10	10,000		$2.3 \pm .56 \times 10^{-7}$		1.2×10^{-6} (Zhang et al., 2011)	23 (Al-Sadi et al., 2011) 17.8 (Zhang et al., 2011)	9–10
FITC-dextran 40	40,000		$8.9 \pm 3.3 \times 10^{-8}$		$.47 \times 10^{-6}$ (Zhang et al., 2011)	46 (Zhang et al., 2011)	9.1
FITC-dextran 70	70,000		$7.4 \pm 2.3 \times 10^{-8}$		$.37 \times 10^{-6}$ (Zhang et al., 2011)	58 (Zhang et al., 2011)	6.7

* S–E eqn = Stokes Einstein equation. Remainder of abbreviations is in the text.

junctions by disruption of cytoskeletal attachment to the tight junctions and downregulation of claudin and occludin (Peixoto and Collares-Buzato, 2005). Dexamethasone up-regulates claudin and occludin among other mechanisms, tightening the tight junction and potentially decreasing permeability.(Shi and Zheng, 2005) We found that serum-free conditions did not alter mannitol permeability despite several days of culture, nor did prolonged (days) exposure to dexamethazone (Fig. 3D). Protamine however significantly increased permeability within several minutes of drug application (Fig. 3D).

Gap junctions. 18β-GA caused an increase in permeability rapidly as well in a dose-dependent manner (Fig. 3A–C). 18β-GA is thought to disassemble gap-junction plaques via a protein phosphatase-mediated dephosphorylation (Guan et al., 1996). Effect was seen within 10 min of drug application resulting in an approximately three-fold increase in mannitol permeability. The effect plateaued in approximately 30 min.

Calcium

Calcium is known to be important in the regulation of the adherens junctions and the tight junctions (Brown and Davis, 2002). Increasing extracellular calcium up to 10 mM did not increase the TEER nor the permeability of mannitol. However, extracellular chelation with EDTA resulted in an increase in permeability consistent with

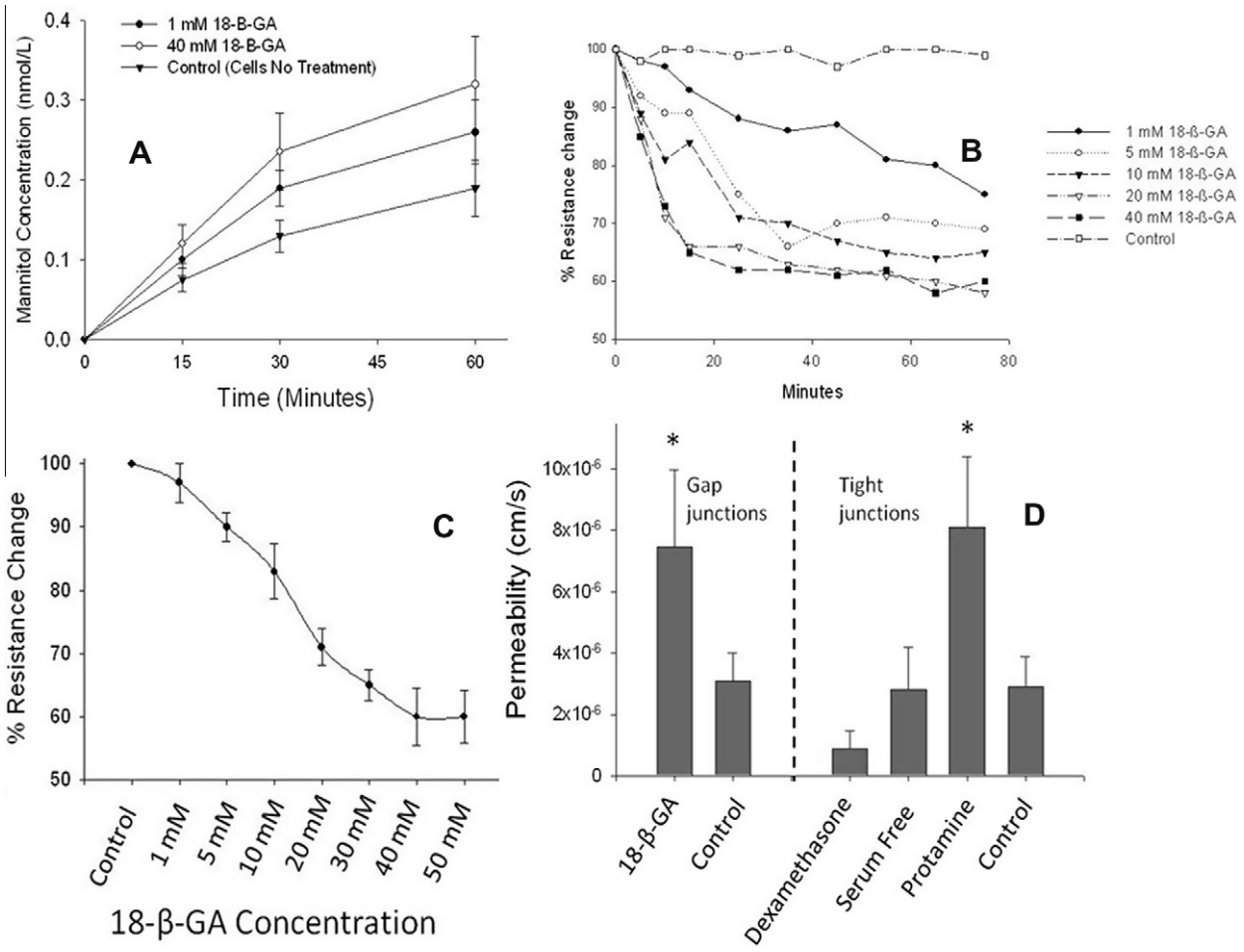

Fig. 3. Perturbation of junctional proteins on arachnoid paracellular transport. (A) 18-β-GA disrupted barrier properties of the arachnoid (*t*-test $p = .045$). Permeability curves of paracellular tracer, mannitol, altered by variable concentrations of 18-β-GA. (B) Effect of 18-β-GA began almost immediately and plateaued at about 30 min. (C) 18-β-GA appears to alter permeability in a dose-response manner as manifested by TEER (D) Dexamethazone, serum-free conditions have minimal effect on mannitol permeability while protamine disrupted barrier formation significantly (*t*-test $p = 0.042$). Error bars denote S.E.

other junctional models such as MDCK (Grebenkämper and Galla, 1994)(Fig. 4A). Chelation effects occurred within 15 min of drug addiction, and were dose dependent (Fig. 4B, C). Effects were persistent until reversal by the washing of the cells with normal media. Tight junction also depends on the intracellular calcium as a second messenger for modulation. We disrupted the intracellular stores by two means: blockage of the transcellular calcium communication and opening the cell membrane to calcium influx. With the calcium channel blocker, verapamil, we did not alter the permeability of mannitol significantly. When we raise the intracellular calcium stores via ionomycin, permeability increased (Fig. 4D). This is consistent with data that suggest tight junction formation is disrupted only by certain intracellular compartments (Stuart et al., 1996), or that higher intracellular calcium concentration is needed for paracellular space regulation.

cAMP

cAMP is known as a second messenger that prevents increased endothelial permeability under the influence of permeability augmenters (Schmidt et al., 2001)(Harrington et al., 2003). We looked at the role of cAMP alone on the effects on paracellular transport and did not find a change in the TEER nor the mannitol permeability. Rolipram, a PDE4 inhibitor, increased the intracellular cAMP and caused a significant decrease in permeability. Likewise, the beta 1,2 agonist, isoproterenol decreased permeability (Fig. 5A). When used in combination, isoproterenol and rolipram did not cause a more pronounced effect nor did isoproterenol and forskolin, a direct adenylyl cyclase agonist. Also, the TEER did not change (Fig. 5B). This may indicate a ceiling effect in the cAMP pathway. Forskolin alone and forskolin and rolipram did not induce much change in the paracellular permeability (Fig. 5C). Application of cAMP modifiers did not alter actin or tight junction protein expression (Fig. 5E, F).

DISCUSSION

The barriers that surround the central nervous system are critical for its homeostasis and its protection. While the BBB has been investigated intensively, only recently

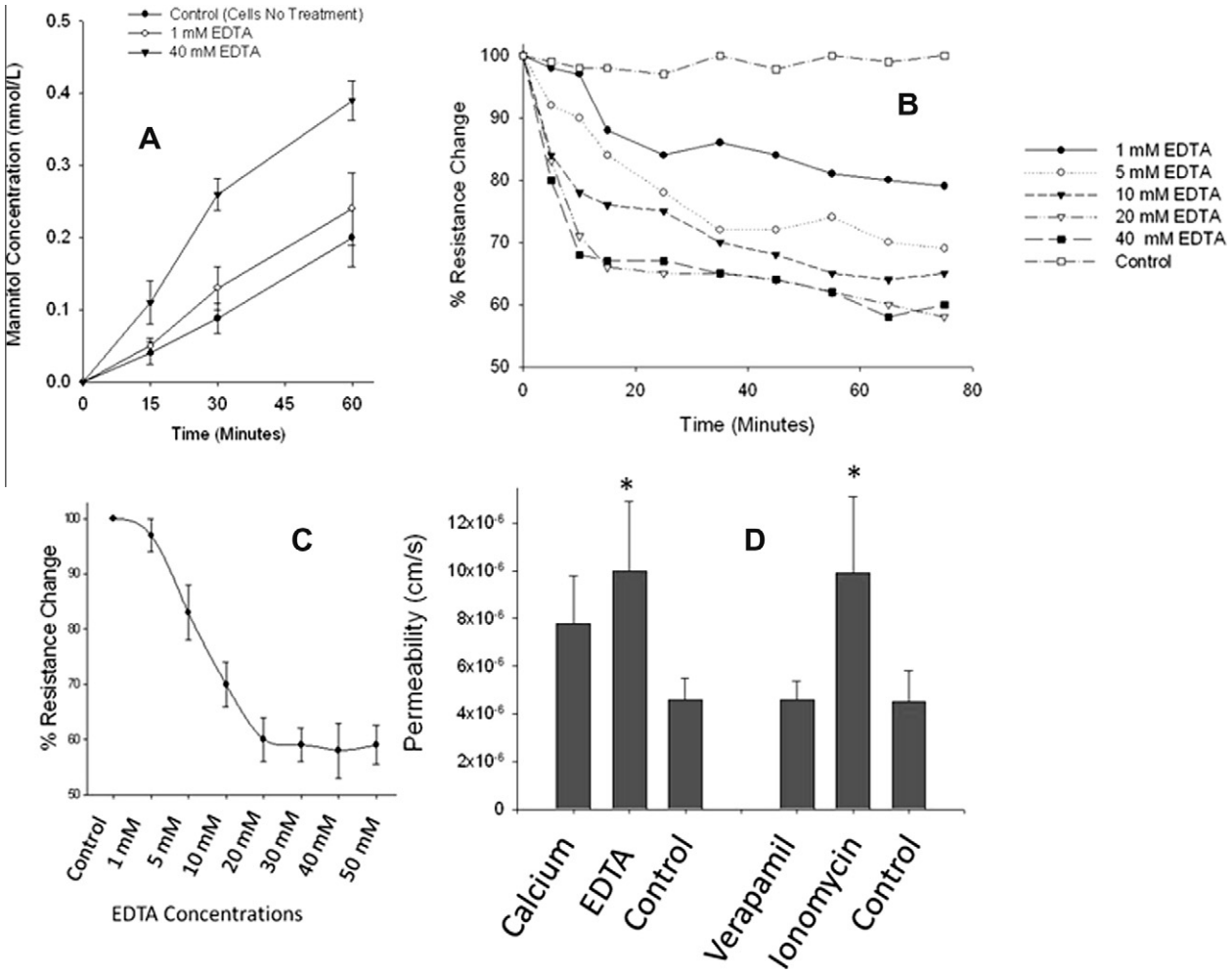

Fig. 4. Calcium modulation of arachnoid. (A) Permeability curves demonstrating differential transport of mannitol with 1 and 40 mM EDTA. (B) Effect appears to begin almost immediately with maximal effect in the first 15 min and all dosing. (C) Dose-response curve at 30 min from application of EDTA from 1 to 50 mM showing TEER change. Maximal change occurs at about 20 mM. (D) EDTA permeability was significantly higher than control (*t*-test $p = 0.041$). Ionomycin had similar effects on paracellular transport (data not shown) and also caused significantly higher permeabilities ($p = 0.043$), while extracellular calcium and verapamil had no difference from control. Error bars denote S.E.

has much attention been paid to the blood-CSF barrier. Even so, the focus has been on the production side of CSF, namely at the choroid plexus, but the gateway to the egress of CSF and the interface of blood to the CSF at the arachnoid granulations and other intracranial structures has largely been ignored. We have previously developed an immortalized cell line of arachnoid cell (Janson et al., 2011) and demonstrated that the arachnoid in monolayers form barriers similar to monolayer models of the BBB (Lam et al., 2011). Immortalized cells are useful but limited in that their properties could be altered in their creation. However, they provide a standardized ready substrate for analysis. Because of the importance of the paracellular transport to the blood-CSF-barrier, we focused on characterizing the extracellular component of the arachnoid-CSF sink. An established tool in BBB research is the utilization of semi-permeable membranes for determining material transport. This method demands that the cells grow on the membrane and can become confluent. There have been successful models of many organs, from intestinal to skin epithelial cells (Li et al., 2004; van de Kerkhof et al., 2007). Even choroid plexus cells have been modeled using this method (Gath et al., 1997; Haselbach et al., 2001). We expanded on the preliminary arachnoid transport data previously reported (Janson et al., 2011) using this technique. The technology intrinsically is flawed despite its widespread use, as the environment in which the cells grow is artificial and does not duplicate the natural environment. Furthermore, arachnoid cells exist in many forms: membranes sparsely populated by cells to densely populated closely packed cells at the arachnoid cap. Nevertheless, the technique permits analysis of the cells on equal footing in comparison to other well-known cell models.

Paracellular transport studies

Dextran. Previous studies have indicated that the paracellular junction does not permit free passage of

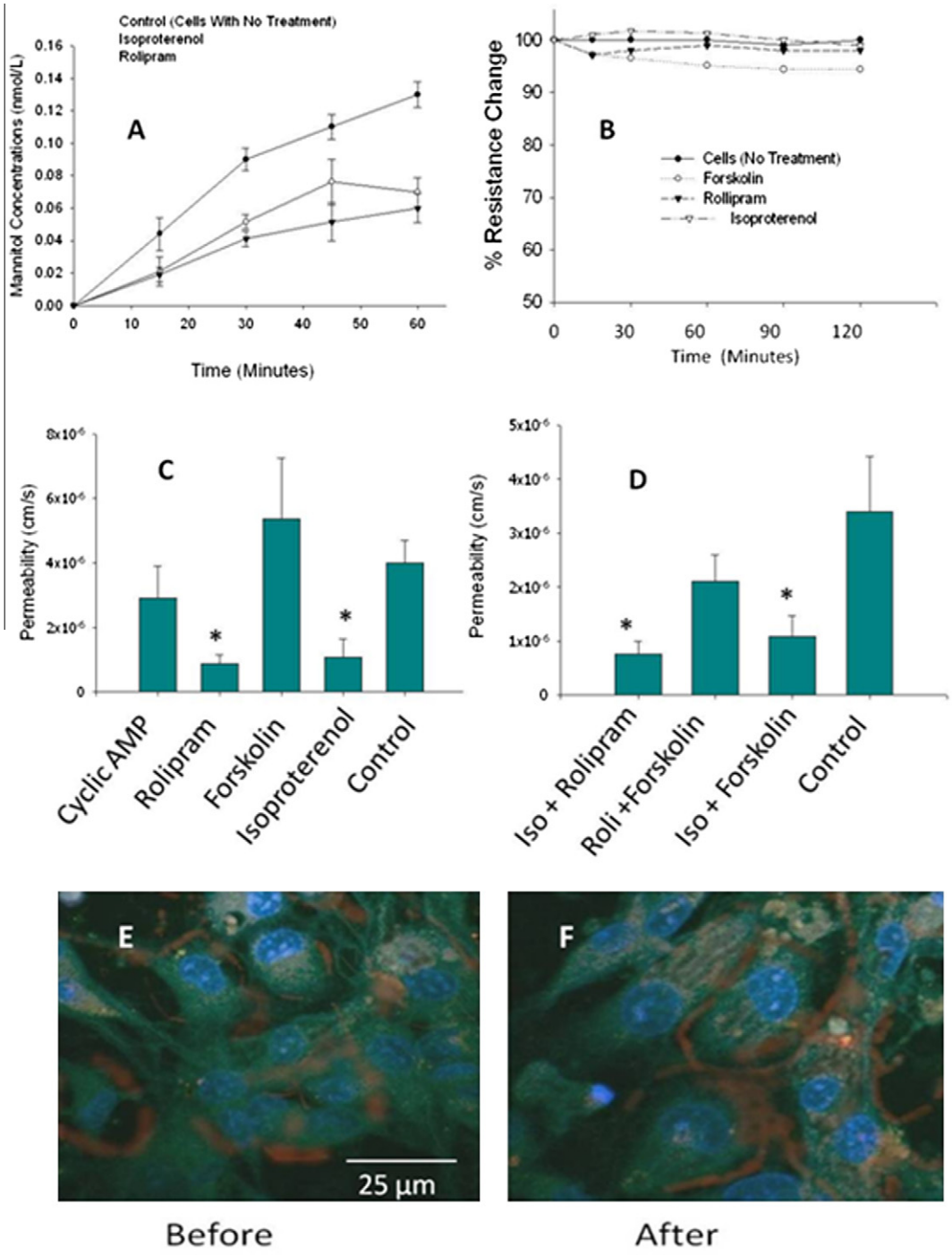

Fig. 5. cAMP modulation of arachnoid permeability. (A) Permeability curves demonstrating differential transport of mannitol with Rolipram and Isoproterenol. (error bars denote standard error) (B) TEER showed minimal change with Forskolin (50 µM), rolipram (10 µM) and isoproterenol (10 µM). Experiments were carried out to 48 h without change in the trend (data not shown) (C) cAMP added into media and forskolin induced minimal changes to mannitol permeability while rolipram and isoproterenol decreased permeability significantly (t test, $p = 0.020$ and 0.024 respectively). (D) When drugs were used in combination, permeability did not decrease further (asterisks signify $p < 0.05$). (E) Before and (F) After addition of isoproterenol and rolipram showed similar appearance in ZO-1 (red) and actin (green) staining.

macromolecules of 3 nm through the interendothelial junctions (Vandenbroucke et al., 2008). If this is the case, then the passage of higher molecular weight dextran should not occur or that its transfer is intracellular. Others have demonstrated this vesicular transfer in the arachnoid cells in native tissue, (Gomez et al., 1974) but in culture, complete transcellular (apical to basal) transport does not occur. (Holman et al., 2010) We utilize this fact to determine the molecular size limit by paracellular movement. We know that in caco-2 cells, macromolecules may pass through monolayers with permeability coefficients two orders of magnitude

smaller than the standard paracellular tracers.(Al-Sadi et al., 2011) Using the same paradigm, dextran over a wide geometric and molecular weight range was used, demonstrating that at the size of approximately 20,000 Da, transport rate slowed markedly. Similar to caco-2, the permeability changed over an order of magnitude, which clarified the mark at which the blood-CSF barrier lies.

Equivalent pore size calculation

Determination for the theoretical pore size is useful in characterizing paracellular transport. It incorporates features of the paracellular space including tortuosity, gap width, cell height, lateral spaces and various junctional protein hindrances (Knipp et al., 1997; Seki et al., 2006). While of limited anatomic accuracy, pore size can use charge, molecular radius, and other rate-determining physicochemical properties to help predict permeability of various substances. We first determined the validity of using this calculation by determining size limitations of the paracellular space. The Renkin hindrance equation is valid for r/R under 0.4, because otherwise, the ratio can exaggerate the diffusional resistance and underestimate pore radius otherwise. Using paracellular markers of neutral p*K*a for experimental determination would decrease solute to pore wall interactions. Our calculation of approximately 11 Å indicates that the pore size to be larger than the caco-2 cells (∼5.2 Å)(Knipp et al., 1997).

Tight junction importance

Our attempt at direct alterations of the tight junction resulted in variable changes in the paracellular tracer permeabilities. Steroid, an upregulator of claudin in other barrier models caused marginal effects on the arachnoid paracellular permeability. It is possible that we are seeing a ceiling effect due to the limitations of other components in the tight junction that prevent increases in the barrier tightness. When we used serum-free conditions, very little changed in the permeability as well. When the serum is withdrawn from culture media, the TEER in cerebral capillary endothelial cells increases, probably due to nonspecific re-organization of the tight junctions (Hoheisel et al., 1998). We found that protamine, which disrupts the cytoskeletal actin distribution and decreases claudin, occludin, and potentially ZO-1 expression, exerts the most effect on the paracellular barrier. Because of the poly cationic nature of protamine, its action on the tight junction is nonspecific (Peixoto and Collares-Buzato, 2005). Together, the evidence suggests that tight junctions by themselves in arachnoid may not be the only important component to the barrier formation. We found that 18β-glycyrrhetinic acid, which binds on connexin at the gap junction had a profound effect on the paracellular permeability in arachnoid. Whether the cause is a mechanical disruption due to the separation of the gap junction, or whether there is a loss of the cell-cell communication that occurs through gap junctions, i.e. calcium transfer, is unknown.

Calcium

In order to determine some of the regulatory mechanisms of the tight junction, we studied two second messenger systems known to alter paracellular transport. Calcium and cAMP have a myriad of effects on the cell, but both are known to impact on tight junctions in other barrier models. Calcium is a second messenger for PKC, but PKC effect on paracellular permeability is variable (Balda et al., 1993; Bazzoni and Dejana, 2004). PKC activation helps assemble the tight junctions but can impair established junctional integrity (Bazzoni, 2006). The PKCα isoform mediates disassembly via actin-mediated cell contraction and is calcium and DAG-dependent (Sandoval et al., 2001; Tiruppathi et al., 2002; Holinstat et al., 2006) PKCβ, also calcium and DAG-dependent, increases the endothelial permeability (Yuan, 2002) as indicated by PKC beta 1 gene transfer in a microvascular endothelial cell line (Nagpala et al., 1996). Intracellular calcium is considered a key regulator in cell contraction and junctional disassembly (Goeckeler and Wysolmerski, 1995; Moy et al., 1996) and is increased with release from the endoplasmic reticulum stores (Mehta and Malik, 2006). Tight junction modulation by intracellular calcium may also proceed via alterations in the subcellular localization of occludin (Ye et al., 1999). We found that the addition of calcium to the extracellular solution did not change the arachnoid cell permeability. Furthermore, blocking calcium from entering the cell also did not change the cell behavior. This supports the claim that some other compartment such as the endoplasmic reticulum stores may be the key to permeability regulation. Only by large scale alteration of the intracellular calcium did we find a tracer transport effect. If we disrupt the extracellular/intracellular calcium homeostasis via calcium ion channel drugs, we demonstrated that the paracellular transport increases, most likely because of the large calcium influx into the cell.

We then determined whether the alteration of extracellular calcium has the same impact as intracellular calcium modulation. EDTA was added as a chelator of extracellular calcium. This does not alter ZO-1/actin interactions unlike intracellular calcium, but may affect the cadherin–cadherin linkage via their extracellular domain (Pokutta et al., 1994). Adherens junctions composed of cadherin join homotypically to adjacent cells and are calcium dependent.(Vandenbroucke et al., 2008) via p120-catenin, cadherin furthermore links the adherens junction to the actin cytoskeleton. In the arachnoid cells, the TEER values were decreased by EDTA but not by the intracellular calcium manipulations, suggesting that adherens junctions may have an important role in the arachnoid barrier formation, but extracellular modulation of the tight junction by calcium may not have.

cAMP

cAMP prevents permeability increases by several mediators in some barrier models. (Schmidt et al., 2001; Harrington et al., 2003). By itself when added extracellularly we did not see any change in the TEER or the paracellular transport in arachnoidal cells. When we

inhibited cAMP breakdown, we were able to increase the barrier capability suggesting a more prominent intracellular role. cAMP induces protein kinase A which inhibits RhoA activation and cellular contraction (Qiao et al., 2003). It may have a direct effect on actin rearrangement thereby affecting the intercellular space formation (Qiao et al., 2003). In addition, it can directly activate Epac, a Rap1GEF which enhances VE-cadherin junctional integrity and actin reorganization (Kooistra et al., 2005). When we examined the immunohistologic staining of the arachnoid cell for actin and ZO-1 before and after the application of cAMP modulators, we did not see any gross changes in intensity or variation in staining pattern (Fig. 4E, F). It is possible that the effect is too subtle to be detected in this manner. Other investigators have noted that the cAMP effect is most marked when the drugs were used in combination with other agents in the case for human and bovine brain endothelial cells (Rubin et al., 1991). When Rubin et al. used a combination of astrocyte-cultured media and cAMP, the cAMP permeability response was the greatest. The reason is not completely clear, but we intend to use astrocytic and neurally-derived soluble factors in combination with cAMP agonist as the next step in this second messenger system analysis. Even without the direct contact by these supporting cells in the BCB, it is possible that they may still influence barrier behavior at the arachnoidal level.

TEER is often viewed as a marker for monolayer integrity or barrier tightness. However, its relation to paracellular permeability did not correlate in the cAMP studies (Fig. 4). This phenomenon has been seen in other monolayer models such as the caco-2 cell line (Takahashi et al., 2002; Kimoto et al., 2009). The physiology is not clear; however, it may be that the paracellular space may widen without change in the junctional protein complex structure allowing for this disparity.

cAMP and Ca second messenger systems may not be separate in their control of extracellular transport. Schmidt et al. showed a new calcium signaling pathway that is triggered by cAMP. This pathway is PKA independent and is mediated by a Rap family GTPase (Schmidt et al., 2001). The receptor studied by that group was the adenylyl cyclase-coupled beta2-adrenoceptor; we used isoproterenol, a beta1,2 agonist which showed a modest effect on permeability.

CONCLUSIONS

We show that the arachnoid cell has the molecular hardware and the capability to support paracellular transport. Occludin, claudin-1, JAM, and actin cytoskeletal protein are present in these cells and play a variable role in transport. The theoretical pore size representing the paracellular space indicates that the gap is wider than other vascular endothelial cell models of the brain. Permeabilities for urea, mannitol and inulin are similar to other models of brain barriers, and the size-differentiated transport of dextran clarified the previously known restriction of soluble dye transport in the blood-CSF barrier at the arachnoid ''sink''. Furthermore, the dextran study indicates that in a standard membrane delimited diffusion system, the efficiency of intracellular transport is approximately one to two orders of magnitude less efficient than paracellular means. We also show that the paracellular transport may be under the influence of both gap junction and tight junctions, and that the calcium and cAMP second messenger systems influence this system. Intracellular and extracellular calcium both appear to have differential roles in increasing the paracellular permeability, and intracellular cAMP is able to decrease the paracellular permeability.

Acknowledgements—The work is funded in part by the ''What-if'' campaign of the University of Minnesota Biomedical Engineering Institute, MN Veterans Medical Research and Education Foundation, the Regent's scholarship program of the University of Minnesota and the Augustine Endowment for MD-PhD graduate studies. Electron microscopy analysis is courtesy of Dr. Gloria Niehans, Department of Pathology, Minneapolis VA Medical Center.

REFERENCES

Adson A, Raub TJ, Burton PS, Barsuhn CL, Hilgers AR, Audus KL, Ho NF (1994) Quantitative approaches to delineate paracellular diffusion in cultured epithelial cell monolayers. J Pharm Sci 83:1529–1536.

Al-Sadi R, Khatib K, Guo S, Ye D, Youssef M, Ma TY (2011) Occludin regulates macromolecule flux across the intestinal epithelial tight junction barrier. Am J Physiol Gastrointest Liver Physiol 300:G1054–64.

Balda MS, Gonzalez-Mariscal L, Matter K, Cereijido M, Anderson JM (1993) Assembly of the tight junction: the role of diacylglycerol. J Cell Biol 123:293–302.

Bazzoni G (2006) Endothelial tight junctions: permeable barriers of the vessel wall. Thromb Haemost 95:36–42.

Bazzoni G, Dejana E (2004) Endothelial cell-to-cell junctions: molecular organization and role in vascular homeostasis. Physiol Rev 84:869–901.

Brown RC, Davis TP (2002) Calcium modulation of adherens and tight junction function: a potential mechanism for blood-brain barrier disruption after stroke. Stroke 33:1706–1711.

Carpenter MB (1991) Core Text of Neuroanatomy 4 Sub. Williams & Wilkins.

Deli MA (2009) Potential use of tight junction modulators to reversibly open membranous barriers and improve drug delivery. Biochim Biophys Acta 1788:892–910.

Gath U, Hakvoort A, Wegener J, Decker S, Galla HJ (1997) Porcine choroid plexus cells in culture: expression of polarized phenotype, maintenance of barrier properties and apical secretion of CSF-components. Eur J Cell Biol 74:68–78.

Goeckeler ZM, Wysolmerski RB (1995) Myosin light chain kinase-regulated endothelial cell contraction: the relationship between isometric tension, actin polymerization, and myosin phosphorylation. J Cell Biol 130:613–627.

Gomez DG, Potts DG, Deonarine V (1974) Arachnoid granulations of the sheep. Structural and ultrastructural changes with varying pressure differences. Arch Neurol 30:169–175.

Grebenkämper K, Galla HJ (1994) Translational diffusion measurements of a fluorescent phospholipid between MDCK-I cells support the lipid model of the tight junctions. Chem Phys Lipids 71:133–143.

Guan X, Wilson S, Schlender KK, Ruch RJ (1996) Gap-junction disassembly and connexin 43 dephosphorylation induced by 18 beta-glycyrrhetinic acid. Mol Carcinog 16:157–164.

Hakvoort A, Haselbach M, Wegener J, Hoheisel D, Galla HJ (1998) The polarity of choroid plexus epithelial cells in vitro is improved in serum-free medium. J Neurochem 71:1141–1150.

Harrington EO, Brunelle JL, Shannon CJ, Kim ES, Mennella K, Rounds S (2003) Role of protein kinase C isoforms in rat epididymal microvascular endothelial barrier function. Am J Respir Cell Mol Biol 28:626–636.

Hasegawa M, Yamashima T, Kida S, Yamashita J (1997) Membranous ultrastructure of human arachnoid cells. J Neuropathol Exp Neurol 56:1217–1227.

Haselbach M, Wegener J, Decker S, Engelbertz C, Galla HJ (2001) Porcine Choroid plexus epithelial cells in culture: regulation of barrier properties and transport processes. Microsc Res Tech 52:137–152.

Hawkins BT, Davis TP (2005) The blood-brain barrier/neurovascular unit in health and disease. Pharmacol Rev 57:173–185.

Hoheisel D, Nitz T, Franke H, Wegener J, Hakvoort A, Tilling T, Galla HJ (1998) Hydrocortisone reinforces the blood-brain properties in a serum free cell culture system. Biochem Biophys Res Commun 247:312–315.

Holinstat M, Knezevic N, Broman M, Samarel AM, Malik AB, Mehta D (2006) Suppression of RhoA activity by focal adhesion kinase-induced activation of p190RhoGAP: role in regulation of endothelial permeability. J Biol Chem 281:2296–2305.

Holman DW, Kurtcuoglu V, Grzybowski DM (2010) Cerebrospinal fluid dynamics in the human cranial subarachnoid space. An overlooked mediator of cerebral disease. II. In vitro arachnoid outflow model. J R Soc Interface 7:1205–1218.

Izevbigie EB, Gutkind JS, Ray PE (2000) Isoproterenol inhibits fibroblast growth factor-2-induced growth of renal epithelial cells. Pediatr Nephrol 14:726–734.

Janson C, Romanova L, Hansen E, Hubel A, Lam C (2011) Immortalization and functional characterization of rat arachnoid cell lines. Neuroscience 177:23–34.

Karczewski J, Groot J (2000) Molecular physiology and pathophysiology of tight junctions III. Tight junction regulation by intracellular messengers: differences in response within and between epithelia. Am J Physiol Gastrointest Liver Physiol 279:G660–665.

van de Kerkhof EG, de Graaf IAM, Groothuis GMM (2007) In vitro methods to study intestinal drug metabolism. Curr Drug Metab 8:658–675.

Kida S, Yamashima T, Kubota T, Ito H, Yamamoto S (1988) A light and electron microscopic and immunohistochemical study of human arachnoid villi. J Neurosurg 69:429–435.

Kimoto T, Takanashi M, Mukai H, Ogawara K, Kimura T, Higaki K (2009) Effect of adrenergic stimulation on drug absorption via passive diffusion in Caco-2 cells. Int J Pharm 368:31–36.

Knipp GT, Ho NF, Barsuhn CL, Borchardt RT (1997) Paracellular diffusion in Caco-2 cell monolayers: effect of perturbation on the transport of hydrophilic compounds that vary in charge and size. J Pharm Sci 86:1105–1110.

Kooistra MRH, Corada M, Dejana E, Bos JL (2005) Epac1 regulates integrity of endothelial cell junctions through VE-cadherin. FEBS Lett 579:4966–4972.

Lam CH, Hansen EA, Hubel A (2011) Arachnoid cells on culture plates and collagen scaffolds: phenotype and transport properties. Tissue Eng Part A 17:1759–1766.

Lanman RC, Burton JA, Schanker LS (1971) Diffusion coefficients of some 14 C-labeled saccharides of biological interest. Life Sci II 10:803–811.

Li H, Sheppard DN, Hug MJ (2004) Transepithelial electrical measurements with the Using chamber. J Cyst Fibros 3(Suppl 2):123–126.

Liu F, Soares MJ, Audus KL (1997) Permeability properties of monolayers of the human trophoblast cell line BeWo. Am J Physiol 273:C1596–1604.

Mehta D, Malik AB (2006) Signaling mechanisms regulating endothelial permeability. Physiol Rev 86:279–367.

Moy AB, Van Engelenhoven J, Bodmer J, Kamath J, Keese C, Giaever I, Shasby S, Shasby DM (1996) Histamine and thrombin modulate endothelial focal adhesion through centripetal and centrifugal forces. J Clin Invest 97:1020–1027.

Nagpala PG, Malik AB, Vuong PT, Lum H (1996) Protein kinase C beta 1 overexpression augments phorbol ester-induced increase in endothelial permeability. J Cell Physiol 166:249–255.

Patton. WEBMAXC EXTENDED. MaxChelator Available at: <www.stanford.edu/~cpatton/webmaxc/webmaxcE.htm>; 2011 [accessed 12.12.2011].

Peixoto EBMI, Collares-Buzato CB (2005) Protamine-induced epithelial barrier disruption involves rearrangement of cytoskeleton and decreased tight junction-associated protein expression in cultured MDCK strains. Cell Struct Funct 29:165–178.

Pokutta S, Herrenknecht K, Kemler R, Engel J (1994) Conformational changes of the recombinant extracellular domain of E-cadherin upon calcium binding. Eur J Biochem 223:1019–1026.

Qiao J, Huang F, Lum H (2003) PKA inhibits RhoA activation: a protection mechanism against endothelial barrier dysfunction. Am J Physiol Lung Cell Mol Physiol 284:L972–980.

Rubin LL, Hall DE, Porter S, Barbu K, Cannon C, Horner HC, Janatpour M, Liaw CW, Manning K, Morales J (1991) A cell culture model of the blood–brain barrier. J Cell Biol 115:1725–1735.

Sakai M, Noach AB, Blom-Roosemalen MC, de Boer AG, Breimer DD (1994) Absorption enhancement of hydrophilic compounds by verapamil in Caco-2 cell monolayers. Biochem Pharmacol 48:1199–1210.

Sandoval R, Malik AB, Minshall RD, Kouklis P, Ellis CA, Tiruppathi C (2001) Ca(2+) signalling and PKCalpha activate increased endothelial permeability by disassembly of VE-cadherin junctions. J Physiol (Lond) 533:433–445.

Schmidt M, Evellin S, Weernink PA, von Dorp F, Rehmann H, Lomasney JW, Jakobs KH (2001) A new phospholipase-C-calcium signalling pathway mediated by cyclic AMP and a Rap GTPase. Nat Cell Biol 3:1020–1024.

Seki T, Kanbayashi H, Nagao T, Chono S, Tabata Y, Morimoto K (2006) Effect of cationized gelatins on the paracellular transport of drugs through caco-2 cell monolayers. J Pharm Sci 95:1393–1401.

Shi LZ, Zheng W (2005) Establishment of an in vitro brain barrier epithelial transport system for pharmacological and toxicological study. Brain Res 1057:37–48.

Skinner RA, Gibson RM, Rothwell NJ, Pinteaux E, Penny JI (2009) Transport of interleukin-1 across cerebromicrovascular endothelial cells. Br J Pharmacol 156:1115–1123.

Stuart RO, Sun A, Bush KT, Nigam SK (1996) Dependence of epithelial intercellular junction biogenesis on thapsigargin-sensitive intracellular calcium stores. J Biol Chem 271:13636–13641.

Takahashi Y, Kondo H, Yasuda T, Watanabe T, Kobayashi S-I, Yokohama S (2002) Common solubilizers to estimate the Caco-2 transport of poorly water-soluble drugs. Int J Pharm 246:85–94.

Tiruppathi C, Minshall RD, Paria BC, Vogel SM, Malik AB (2002) Role of Ca^{2+} signaling in the regulation of endothelial permeability. Vascul Pharmacol 39:173–185.

Upton ML, Weller RO (1985) The morphology of cerebrospinal fluid drainage pathways in human arachnoid granulations. J Neurosurg 63:867–875.

Vandenbroucke E, Mehta D, Minshall R, Malik AB (2008) Regulation of endothelial junctional permeability. Ann NY Acad Sci 1123:134–145.

Wigham CG, Turner HC, Swan J, Hodson SA (2000) Modulation of corneal endothelial hydration control mechanisms by Rolipram. Pflugers Arch 440:866–870.

Wolpow ER, Schaumburg HH (1972) Structure of the human arachnoid granulation. J Neurosurg 37:724–727.

Ye J, Tsukamoto T, Sun A, Nigam SK (1999) A role for intracellular calcium in tight junction reassembly after ATP depletion-repletion. Am J Physiol 277:F524–532.

Yuan SY (2002) Protein kinase signaling in the modulation of microvascular permeability. Vascul Pharmacol 39:213–223.

Zhang Z, Nadezhina E, Wilkinson KJ (2011) Quantifying diffusion in a biofilm of *Streptococcus* mutans. Antimicrob Agents Chemother 55:1075–1081.

(Accepted 29 June 2012)
(Available online 17 July 2012)